

Vectorial second-harmonic magneto-optic Kerr effect measurements

P. Kabos,^{a)} A. B. Kos, and T. J. Silva

Electromagnetic Technology Division, National Institute of Standards and Technology, Boulder, Colorado 80303

A significant modification of an existing experimental technique based on the second-harmonic magneto-optical Kerr effect (SH-MOKE) is introduced. With a p -polarized pumping optical wave incident upon a magnetic film, the transverse component of magnetization causes a change in the second-harmonic generation efficiency of the material and the longitudinal component of the magnetization produces a change in the polarization rotation and/or ellipticity of the second-harmonic signal. This permits simultaneous vectorial measurement of the in-plane magnetization components. Examples of measured hysteresis loops from 50 nm thick permalloy films and procedures for SH-MOKE signal calibration are presented. [S0021-8979(00)17108-7]

I. INTRODUCTION

In this article we introduce a technique for the vectorial measurement of magnetization applicable to thin films. It is based on a novel modification of the well-established second-harmonic magneto-optic Kerr effect (SH-MOKE) technique. In a SH-MOKE experiment, a sample is illuminated with light at frequency ω , and a signal at frequency 2ω is generated at the surface when the peak power densities exceed about 10 GW/cm^2 . As discussed below, the signal at 2ω is related to the in-plane components of the magnetization vector, permitting the vectorial measurement of magnetization \mathbf{M} . This technique has several advantages. First, SH-MOKE exhibits enormous magnetic contrast, with demonstrated intensity changes of up to 50% (or upto 60% for permalloy).¹ Second, the technique may be used to measure the magnetic behavior in an extremely small sample area because of its surface sensitivity resulting from nonlinear optical origins. Third, subpicosecond time resolution gives a broad dynamic range for the observation of any time-dependent fine structure in the magnetization components' response during the switching process. The modification of the existing SH-MOKE technique should greatly extend its experimental utility.

Berger and Pufall² have demonstrated vector magnetometry with a continuous wave laser source using generalized magneto-optical ellipsometry (GME). Such an approach has the obvious advantage of using an inexpensive light source, as opposed to an ultrafast laser required for SH-MOKE. In addition, GME may be considered a "bulk" sensitive technique, insofar as the depth sensitivity of MOKE greatly exceeds that of SH-MOKE. We consider GME and the nonlinear optical method outlined here to be complementary. However, GME does require multiple measurements at different settings of the polarizer and analyzer for a given magnetization state for a unique determination of the magnetization vector. The method described here relies on a simultaneous determination of both the polarization and intensity of second-harmonic light, a process that is more conducive to dynamical measurements.

II. METHOD

A sample of permalloy ($\text{Ni}_{81}\text{Fe}_{19}$) film, 50 nm thick, grown on Si by dc magnetron sputtering was positioned on a holder. Two sets of Helmholtz coils were positioned around the holder to provide two orthogonal magnetic fields in the plane of the sample for static bias or for static measurement of hysteresis loops.

The following coordinate conventions will be used throughout the article: The film defined the x - y plane. The incident laser beam defined the x - z plane, with the z axis normal to the film plane. The magnetization components in the x and y axes are referred to as the longitudinal and transverse components, respectively. For these measurements, the film was magnetized in the plane of the film. The out-of-plane or z component of magnetization can be neglected in this particular case; this assumption is well justified for permalloy films several tens of nanometers thick and with a saturation magnetization of 800 kA/m .

Second-harmonic generation (SHG) from a metallic surface may be described with a phenomenological second-order reflectivity tensor, where the basis coordinates of the incident electric field are either in the plane of incidence (p) or orthogonal to it (s). The SHG is then given by

$$\begin{bmatrix} E_s(2\omega) \\ E_p(2\omega) \end{bmatrix} = \begin{bmatrix} r_{ss}^{(2)} & r_{sp}^{(2)} \\ r_{ps}^{(2)} & r_{pp}^{(2)} \end{bmatrix} \begin{bmatrix} E_s(\omega) \\ E_p(\omega) \end{bmatrix}. \quad (1)$$

Both in-plane magnetization components contribute to the SH-MOKE signal. In the case of $E_s(\omega)=0$ (p incidence), the transverse magnetization component M_y contributes only to the second-order Fresnel reflection coefficient $r_{pp}^{(2)}$, while the second-order reflection coefficient in the s direction $r_{sp}^{(2)}$ is unaffected.³ Hence, in the p -transverse geometry, the change in the transverse magnetization component contributes only to a change of the SHG efficiency. However, the longitudinal magnetization component M_x contributes primarily to $r_{sp}^{(2)}$; in a first-order approximation $r_{pp}^{(2)}$ remains unaffected by M_x . In addition, $r_{sp}^{(2)}$ exhibits purely odd dependence on M_x , changing its sign with the changing direction of M_x . Any change in rotation of the polarization and/or ellipticity of the signal can, therefore, be attributed entirely to the longitudinal magnetization component.

^{a)}Electronic mail: kabos@lamar.colostate.edu

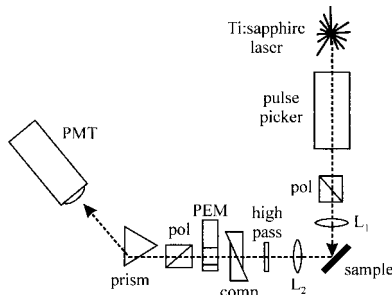


FIG. 1. Block diagram of the measurement.

In general, longitudinal SH-MOKE also results in a change of SHG efficiency. However, for permalloy at a 45° angle of incidence longitudinal SH-MOKE is less than 10%,⁴ resulting in a net change in SHG of only 1%–2%. Such a small change in intensity may be neglected if compared with the enormous magnitude of change in intensity (~ 60%) for transverse SH-MOKE. The potential for much larger change in polarization in the case of longitudinal SH-MOKE merits caution in adopting these methods to arbitrary materials, especially at small angles of incidence.⁵ These two manifestations of SH-MOKE permit simultaneous vectorial measurement of the in-plane magnetization.

III. EXPERIMENTAL SETUP

A block diagram of the measurement is shown in Fig. 1. As a laser source, we used a commercial mode-locked Ti:sapphire laser producing pulses 50–60 fs long, with an 82 MHz repetition rate at an 800 nm wavelength. The pulse-repetition rate was reduced to 1 MHz by use of a commercial electro-optic “pulse picker,” thereby reducing the average power incident on the sample to 4–5 mW without sacrificing the high peak power densities required for SHG. This allowed us to use a much smaller spot size at the sample than would otherwise be possible. P-polarized light was incident on the sample at an angle of 45°, and was focused to spot size of approximately 5 μm. After reflection from the sample surface, the light was collimated by a second lens and passed through the first level of filtration by an interference filter designed to remove the fundamental frequency of the light from the SHG. The second-harmonic signal was then directed successively into a Babinet–Soliel compensator, a photoelastic modulator (PEM), an analyzer set at 45°, a triangular prism to further filter out the fundamental light, and then a photomultiplier tube (PMT) operated in photon counting mode. A coincidence-detection circuit selected only those photon-induced pulses that were coincident with the laser pulses, thereby greatly reducing the detected background signal. The resulting digital pulses are then fed simultaneously to a digital counter and a lock-in amplifier.

The combination of the PEM, analyzer, and lock-in amplifier measured the SHG ellipticity and/or polarization angle.⁶ The signals at the fundamental component of the PEM modulation frequency (50 kHz) and at the second harmonic of the modulation frequency correspond to the ellipticity and the polarization rotation, respectively. Both signals may be used for the measurement. We used the compensator to convert all polarization changes into angular rotations, thereby simplifying the measurement.

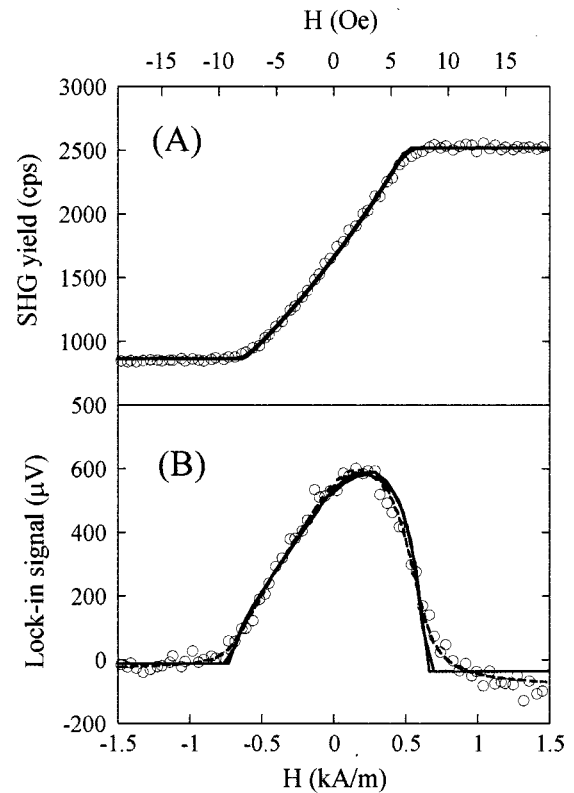


FIG. 2. As measured SH-MOKE signals corresponding to (A) the photon counteroutput and (B) the lock-in amplifier signal. The sample was a permalloy film 50 nm thick on Si with uniaxial anisotropy along the *x* axis. The solid lines drawn through the data are the fits using SW to model the dependence of *M* on *H*. The dashed line in (B) is the fit with 24 A/m (0.3 Oe) of stray longitudinal (*x*-axis) field included in the model.

IV. RESULTS AND DISCUSSION

Figure 2 shows the raw hysteresis-loop signals corresponding to the digital counter output (A) and the lock-in amplifier output (B) for a permalloy film 50 nm thick. The swept magnetic field was orthogonal to the easy, *x* axis of the sample. The digital counter signal was a direct measurement of transverse SH-MOKE, corresponding to *M_y*, while the lock-in signal comprised a mixture of longitudinal and transverse SH-MOKE, insofar as the lock-in output is proportional to both the polarization angle and the intensity of the SHG yield. This requires normalization of the lock-in signal by the SHG signal seen in Fig. 2(A) to obtain the pure longitudinal SH-MOKE signal.

To obtain the magnetization components from the raw data, we employed a calibration procedure similar to the one described in Ref. 7. The transverse SH-MOKE signal is equal to

$$I = \frac{I_0}{|\chi_{nm}^{(2)}|^2} (|\chi_{nm}^{(2)}|^2 + |\chi_m^{(2)}|^2) m_y^2 + 2 \cos \phi |\chi_{nm}^{(2)}| |\chi_m^{(2)}| m_y^2, \quad (2)$$

where we have decomposed the effective second-order susceptibility tensor component $\chi_{nm}^{(2)}$ into its magnetically sensitive ($\chi_m^{(2)}$) and insensitive ($\chi_{nm}^{(2)}$) parts. *I*₀ is the SHG intensity due solely to nonmagnetic source terms. The phase

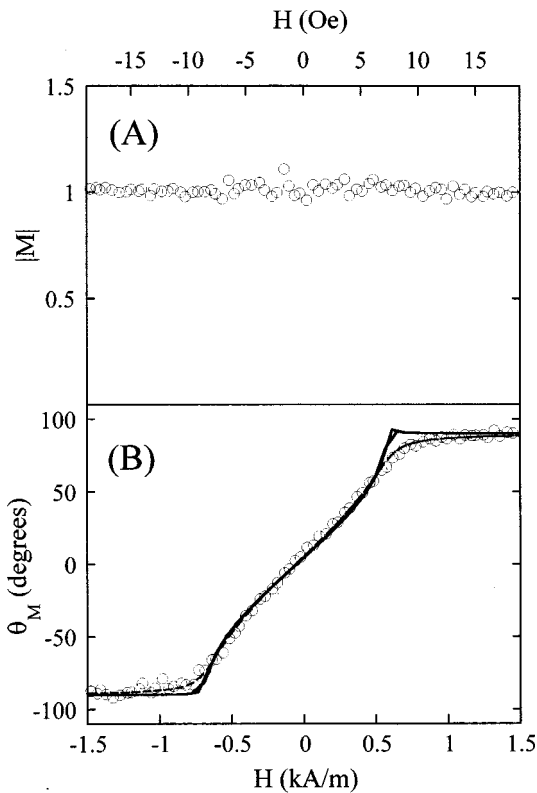


FIG. 3. Processed experimental data with the (A) magnetization magnitude $|M|$ and (B) magnetization angle θ_M as functions of external field. The sample was a permalloy film 50 nm thick on Si with uniaxial anisotropy along the x axis. The solid line represents the SW fit to the data *after calibration*. The dashed line in (B) is the SW fit with 24 A/m (0.3 Oe) of stray longitudinal (x -axis) field included in the model $H_k = 640$ A/m (8 Oe), as determined from the SW fit.

difference between $\chi_{nm}^{(2)}$ and $\chi_m^{(2)}$ is given by ϕ , and $m_y = M_y/M_x$. We model the field dependence of m_y with the Stoner–Wohlfarth (SW) equation for a single-domain uniaxial-anisotropy system. Nonlinear least-squares fitting to the data permits extraction of $|\chi_{nm}^{(2)}|/|\chi_m^{(2)}|$, ϕ , and I_0 . Determination of these four parameters thereby provides the calibration of the transverse SH-MOKE measurements: We solve for m_y as a function of I using Eq. (2). The longitudinal SH-MOKE data (i.e., the lock-in signal divided by the countersignal) are assumed to be linear in M_x . The proportionality constants are determined by fitting experimental data to SW calculations.

The solid lines in Fig. 2 show the results of fitting. The fit to transverse SH-MOKE in Fig. 2(A) is excellent. However, at positive H there is some discrepancy between lock-in data and the fit curve: The data exhibit a smooth approach to saturation, whereas the SW model predicts sharp saturation at $H = H_k$. This slight departure from exact SW behavior is most likely the effect of a stray magnetic field directed along the easy axis that was not completely cancelled out by the Helmholtz coils. For illustration of this point we have included a fit to the data in Fig. 2(B) with only 24 A/m (0.3 Oe) of stray easy-axis field. The addition of this stray field removes the discrepancy between the fit and the data.

Figure 3 shows the results of the calibration procedure for both the normalized average magnetization $|M|$ [Fig. 3(A)] and the magnetization angle θ_M [Fig. 3(B)]. The solid

line is the SW fit to the data *after* calibration of the raw data. Like in the case shown in Fig. 2(B), the fit to θ_M could be improved (dashed line) by inclusion of 24 A/m (0.3 Oe) of stray longitudinal field. Both the magnitudes of “local” anisotropy field, H_k , and orientation, ϵ , can be determined with a high degree of accuracy from this subsequent fit. Figure 3(A) represented a self-consistency check of the technique: Within experimental error the resulting average magnetization is equal to unity over the applied field interval. From Fig. 3, one may conclude that the magnetization process for our particular sample is reasonably well described by the coherent rotation model of SW.

As was discussed above, the fitting procedure gives the ratio of the effective magnetic and nonmagnetic second-order susceptibility components $\chi_r = |\chi_{nm}^{(2)}|/|\chi_m^{(2)}|$, as well as the local anisotropy field H_k . For the spot measured in Fig. 3 the particular values were $H_k = 640$ A/m \pm 8 A/m (8 Oe \pm 0.1 Oe), $\epsilon = 0.14^\circ \pm 0.08^\circ$, $\chi_r = 0.27$, and $\phi = 0.002$.

We were therefore able to map spatial variations in both the magnetic and nonlinear optical properties. As an example, we determined the variation of the local anisotropy field magnitude and angle obtained from a second sample with a permalloy film 50 nm thick deposited on a 100 μ m sapphire substrate. We observed a noticeable positional variation of the anisotropy field in the investigated sample, suggesting the presence of a magnetization ripple.^{8,9} The standard deviation of the anisotropy magnitude and angle were 13.6 A/m (0.17 Oe) and 2.4° , respectively. The measured variation of H_k exceeded the error estimates at the individual points by a factor of ~ 2 , indicating that the technique has a sufficient signal-to-noise ratio to resolve the local variations of anisotropy. Such spot measurements more directly determine *the source* of the magnetization ripple (i.e., dispersion in H_k) than bulk magnetometry techniques, such as transverse-bias permeability or inductive-looper measurements.

In conclusion, we have introduced an experimental technique that allows vectorial measurements of in-plane components of magnetization in thin films. This method proved to be useful for determination of magnetization reversal processes in the thin-film magnetic structures, and can also provide definitive experimental verification of different theoretical models due to its vectorial nature. We presented examples of only static vectorial SH-MOKE measurements; however, this technique is also amenable to dynamic measurements, insofar as the use of a pulsed laser permits optical sampling of magnetic response.¹⁰

¹T. M. Crawford, C. T. Rogers, T. J. Silva, and Y. K. Kim, Appl. Phys. Lett. **68**, 1573 (1996).

²A. Berger and M. R. Pufall, J. Appl. Phys. **85**, 4583 (1999).

³T. M. Crawford, Ph.D. thesis, University of Colorado, Boulder, 1995.

⁴T. M. Crawford, C. T. Rogers, T. J. Silva, and Y. K. Kim, IEEE Trans. Magn. **32**, 4087 (1996).

⁵B. Koopmans, M. G. Koerkamp, T. Rasing, and H. van den Berg, Phys. Rev. Lett. **74**, 3692 (1995).

⁶F. Suits, IEEE Trans. Magn. **28**, 2976 (1992).

⁷T. J. Silva and T. M. Crawford, IEEE Trans. Magn. **35**, 671 (1999).

⁸K. J. Harte, J. Appl. Phys. **39**, 1503 (1968).

⁹H. Hoffmann, IEEE Trans. Magn. **4**, 32 (1968).

¹⁰T. M. Crawford, T. J. Silva, C. W. Teplin, and C. T. Rogers, Appl. Phys. Lett. **74**, 3386 (1999).